Jurnal Kejuruteraan 36(3) 2024: 1005–1020
https://doi.org/10.17576/jkukm-2024-36(3)-15

Investigation of GeSe Photovoltaic Device Performance via 1-Dimensional Computational Modelling

Wong Wei Lii[a,b], Badariah Bais[a,b*], Kazi Sajedur Rahman[c] & Puvaneswaran Chelvanathan[c*]

[a]*Electrical and Electronic Engineering Programme,*

[b]*Department of Electrical, Electronic and Systems Engineering, Faculty of Engineering & Built Environment, Universiti Kebangsaan Malaysia, Malaysia*

[c]*Solar Energy Research Institute, Universiti Kebangsaan Malaysia, Malaysia*

[*]*Corresponding author: badariah@ukm.edu.my; cpuvaneswaran@ukm.edu.my*

Received 30 July 2023, Received in revised form 19 October 2023
Accepted 19 November 2023, Available online 30 May 2024

ABSTRACT

Germanium selenide (GeSe) is a potential absorber material for thin film solar cells. However, many physical, electronic parameters and practical defect configurations that result in different effects on the performance of GeSe solar cells are not fully understood. In this study, a baseline of a GeSe thin film solar cell was designed and simulated using SCAPS-1D simulator. The physical and electronic parameters of the absorber layer is varied to investigate their effect on the performance of the solar cell. The simulation uses absorption files extracted from Xue et al. 2016 and the SCAPS-1D absorption model. Practical defect configurations are also introduced in GeSe thin film solar cells to optimize solar cell performance. Simulation results show that baseline GeSe solar cells had obtained Voc 0.62 V, Jsc 39.52 mA/cm^2, FF 79.34 and η 19.48%. Simulation using the SCAPS-1D absorption model achieved a more accurate J_{SC} contour graph compared to simulation using absorption files extracted from Xue et al. 2016. The highest efficiency of 26.13% was achieved at 1.40 eV bandgap, 4.27 eV electron affinity, 10 cm^2/Vs hole mobility, 1E +18 1/cm^3 hole concentration and 2000 nm GeSe layer thickness. For bulk defect, an increase in defect concentrations or capture cross section hole and electron (σ) reduce efficiency. For interfacial defect GeSe/CdS, total density of 1E+12 1/cm^2 with σ of 1E-13 cm^2, total density of 1E+18 1/cm^2 with σ of 1E-19 cm^2, total density of 1E+16 1/cm^2 and 1E+18 1/cm^2 with σ of 1E-16 cm^2 have critical impact to solar cell.

Keywords: GeSe thin film solar cell; bandgap; electron affinity; hole mobility; hole concentration; thickness; defect

INTRODUCTION

Solar energy is energy produced by the sun's radiation and it is a renewable energy source that can be used to produce electricity, heat water, etc. Solar energy has become increasingly popular in recent years because it can reduce dependence on fossil fuels and carbon emissions. Photovoltaics is the process of converting energy from sunlight into electricity. The photovoltaic process is carried out using photovoltaic cells, also known as solar cells. China is one of the countries that extensively uses solar cells. The country has invested heavily in developing and deploying solar energy technology, particularly large-scale solar power plants. As a result, China has the highest solar energy capacity in the world and is responsible for producing a significant portion of the world's solar panels.

The p-n junction cell is one of the most common solar cells. The junction of a p-type semiconductor and an n-type semiconductor forms the p-n junction. A p-type semiconductor is created by adding an impurity such as boron, which has one less electron in its outermost energy level than the semiconductor material. This creates holes in the lattice structure, through which electrons are lost. An n-type semiconductor is created by adding an impurity

such as phosphorus, which has one more electron in its outermost energy level than the semiconductor material. This creates an excess of electrons in the lattice structure. When a p-n junction is created, electrons from the n-type side flow into holes on the p-type side, creating a depletion region. This region acts as a barrier to further electron flow and creates a built-in electric field. When light is absorbed by a solar cell, it can excite electrons in the depletion region to a higher energy level, allowing electrons to flow across the junction and generate electricity. This process is known as the photovoltaic effect (Sze & Ng 2007).

Currently, crystalline-Silicon (c-Si) solar cells, including polycrystalline and monocrystalline Si dominate the photovoltaic (PV) market due to their relatively high-power conversion efficiency (PCE), excellent stability and reliability, and the established Si industry. c-Si solar cells account for about 94% of total annual production. However, due to the low absorption coefficient of Si originating from its indirect band gap, c-Si can only be used for solar cells with a thickness of about 200 μm to absorb most of the incident light. In terms of the use of absorbent materials with high absorption coefficients, thin film solar cells offer the possibility of making flexible devices on flexible substrates such as metals and polyimide films while reducing material consumption. Currently, the representative thin film solar cells are cadmium telluride (CdTe) and copper indium gallium selenide (CIGS). Their PCE has reached 22.1% and 23.4% respectively. Notably, CIGS flexible solar cells grown on polyimide substrates exhibited a PCE of 18.7%, indicating that thin film flexible solar cells with high efficiency comparable to rigid substrate solar cells can be achieved (Liu et al. 2020).

Next-generation absorber materials used in thin film photovoltaics are receiving increasing research interest. This shift is due to the toxicity of Cd and the lack of In and Te found in the best absorbent materials developed, which are cadmium telluride (CdTe) and copper indium gallium diselenide (CIGS). In this aspect, GeSe is a potential candidate as a photovoltaic absorber material for several reasons, such as the abundance of Ge and Se on Earth and their low toxicity. This feature gives it an advantage over CdTe and CIGS, where it requires rare or toxic elements. GeSe also has attractive optical and electrical properties for photovoltaic applications. The first GeSe thin film solar cell was reported by Xue et al. (2016) with η 1.48%. Liu et al. (2021) reported that GeSe solar cells are limited by interface rather than bulk defects. By passivating interface defects, η of 5.2% was obtained. In addition, many factors that can affect the efficiency of solar cells such as band gap, electron affinity, hole mobility, hole concentration, layer thickness, and various types of practical defects that are difficult to control.

Defects in solar cells can manifest in various forms. Typically, these defects have undesired effects, such as reducing the solar cell efficiency (η). However, under certain conditions and specific types of defects, they can enhance solar cell efficiency (η). Defects create traps that influence carrier mobility, contribute to the recombination of charge carriers, and cause electrical degradation (Kearney et al. 2018).

Several types of defects can exist in solar cells, including bulk and interfacial defects. Bulk defects occur within the material itself, which is within the lattice structure. Examples include vacancies (missing atoms in the lattice), interstitial defects (additional atoms occupying positions between lattice sites), or substitution defects (different atoms replacing some original atoms in the lattice). Interfacial defects are a type of defect that occurs at the interface or boundary between two different materials or layers within the solar cell (Karl & Udo 2018).

To analyze the performance of solar cells, there are four important parameters, which are open circuit voltage (Voc), short circuit current density (Jsc), fill factor (FF) and efficiency (η). Voc is the voltage measured across the solar cell when no current is flowing through it and is a measure of the maximum voltage it can produce. Jsc is the current measured across the solar cell when the voltage across the cell is at its minimum and represents the maximum current that can be generated by the solar cell. FF is a measure of the efficiency of the solar cell in converting light to electricity. It is calculated as the ratio of the cell's maximum power output to the product of its Voc and Jsc. η is the percentage of light energy converted into electricity by the solar cell and is calculated as the ratio of the solar cell's maximum power output to the solar power.

METHODOLOGY

MODELLING

SCAPS-1D is a powerful and widely used software tool specially designed for simulating and analyzing the performance of solar cells. It has become a popular software among researchers due to its ability to accurately predict the performance of various solar cell architectures and materials. The accuracy of this software has been verified by comparing its results with actual solar cells. SCAPS-1D employs a comprehensive set of algorithms to calculate solar cell efficiency by considering factors such as optical absorption, carrier transport, device architecture, and the impact of defects on carrier recombination. This software is firmly rooted in semiconductor physics and numerical methods, utilizing theoretical frameworks like

the Shockley-Queisser detailed balance limit and transport equations for charge carriers. By integrating these elements, SCAPS-1D has the capability to design solar cells and simulate the solar cell with various parameters and complex defect profiles, which consist of different types of defects (acceptor, neutral and donor) and energy distributions (single, uniform, Gaussian, CB tail and VB tail). SCAPS-1D also enable users to obtain crucial electronic parameters, including Voc, Jsc, FF, and η. Therefore, SCAPS-1D was chosen as the simulation tool to simulate the performance of solar cells in this study.

Figure 1 shows the methodology for analyzing the performance of solar cells in order to design a GeSe solar cell with high η. The methodology is divided into three phases. The study begins with a literature review to identify parameters and factors that can influence the performance of GeSe solar cells. Data on GeSe solar cell parameters are collected from recent research as references. Additionally, an investigation into practical defect configurations will be conducted. For the first phase, a basic model of GeSe solar cells is developed and simulated using SCAPS 1-D software. The performance of the solar cells is analyzed through open-circuit voltage (Voc), short-circuit current density (Jsc), fill factor (FF), and efficiency (η). In the second phase, the physical and electronic parameters of GeSe will be varied to analyze their effects on solar cell performance. Contour plots will be generated and analyzed based on the data obtained. In the third phase, bulk and interfacial defects were inserted into the solar cells and simulated. The impact of these defects on the solar cell performance were simulated and analyzed.

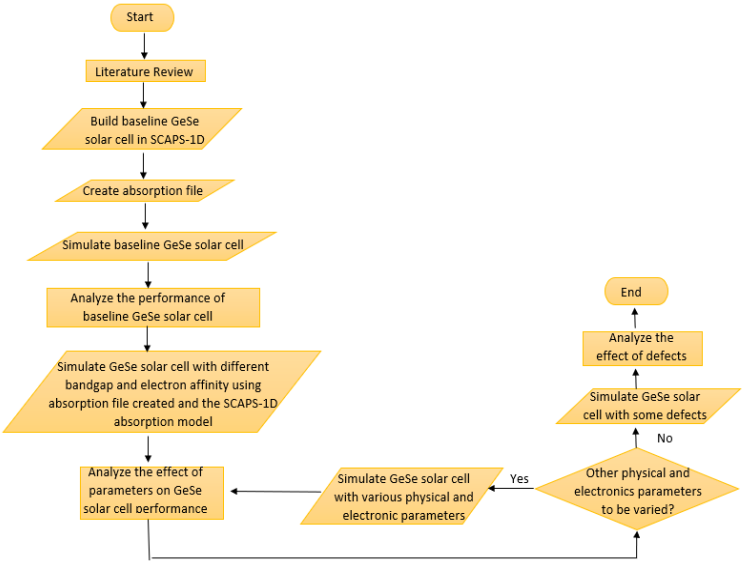

FIGURE 1. Flowchart of the study

PARAMETER OF SOLAR CELL

In this study, a basic structure model of GeSe solar cell is built, as shown in Figure 2. The studied parameters are bandgap, electron affinity, hole concentration, hole mobility and thickness in the GeSe layer. The baseline parameter of the GeSe solar cell is shown in Table 1.

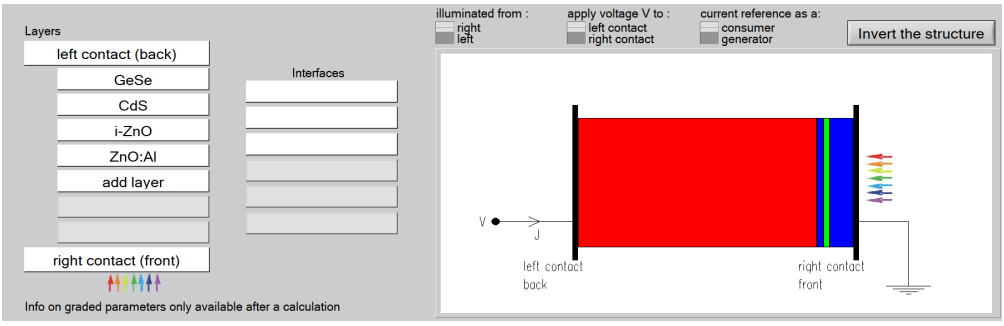

FIGURE 2. The layers in GeSe solar cell

TABLE 1. Baseline parameter of GeSe solar cell

Parameter	ZnO:Al	i-ZnO	CdS	GeSe
Thickness (nm)	200	50	55	1000
Bandgap (eV)	3.3	3.3	2.4	1.14
Electron affinity (eV)	4.4	4.5	4.2	4.09
Dielectric permittivity (relative)	9	9	10	15.3
CB effective density of states (1/cm^3)	2.2E+18	2.2E+18	2.2E+18	3.801E+18
VB effective density of states (1/cm^3)	1.8E+19	1.8E+19	1.8E+19	2.669E+19
Electron thermal velocity (cm/s)	1E+8	1E+8	1E+8	1.739E+7
Hole thermal velocity (cm/s)	1E+8	1E+8	1E+8	9.081E+6
Electron mobility (cm^2/Vs)	1E+3	1E+3	1E+3	40
Hole mobility (cm^2/Vs)	25	25	25	10
Shallow uniform donor density N_D (1/cm^3)	1E+21	1E+19	1.1E+17	0
Shallow uniform acceptor density N_A (1/cm^3)	0	1E+19	0	1E+16

ABSORPTION MODEL

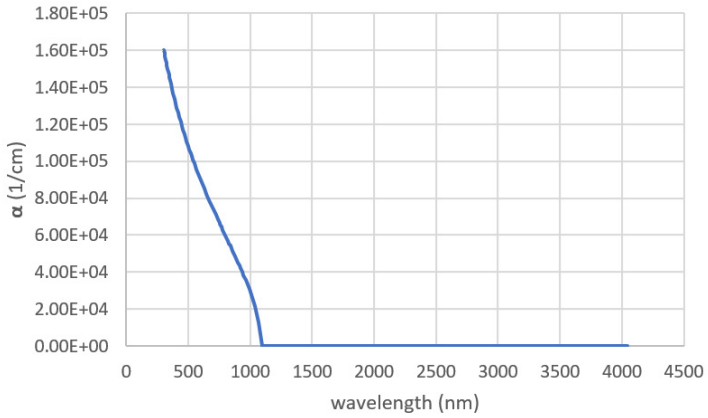

FIGURE 3. SCAPS-1D absorption model

Two absorption models were applied in this study which are the SCAPS-1D absorption model, namely sqrt(hv-Eg) as shown in Figure 3 and absorption files extracted from Xue et al. 2016 as shown in Figure 4.

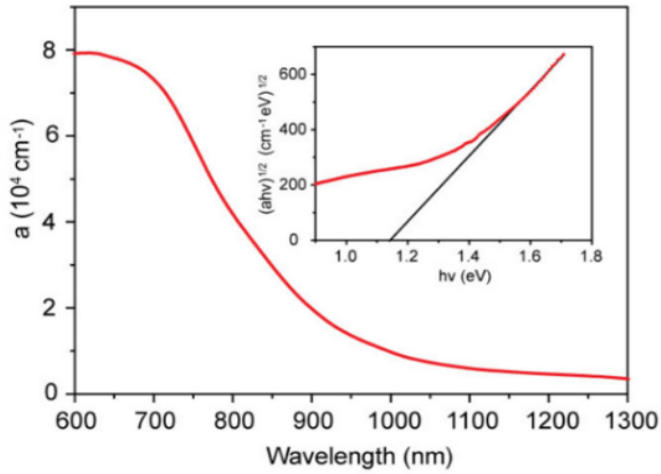

FIGURE 4. Absorption files extracted from Xue et al. 2016

DEFECT PROFILES

Two types of defects were simulated which are bulk defects and interfacial defects. The bulk defect is inserted in the GeSe layer. Three types of bulk defects were simulated, namely Se_{Ge} acceptor defects (H1), Ge_{Se} acceptor defects (H2) and a combination of Se_{Ge} and Ge_{Se} acceptor defects (H1+H2). Simulations were performed by changing the capture cross section hole and electron (σ) from 1E-23 cm^2 to 1E-11 cm^2 and the concentration of defects (N_t). The defect parameter settings are shown in Table 2.

TABLE 2. Bulk defect parameter

Parameter	H1	H2
N_t ($1/cm^3$)	1.3E+12	3.0E+12
	1.3E+14	3.0E+14
	1.3E+16	3.0E+16
	1.3E+18	3.0E+18
Energy with respect to reference (eV)	0.35 above E_v	0.51 above E_v
Defect type	Single Acceptor	Single Acceptor
Energy distribution	Single	Single

An interfacial defect was inserted between the GeSe and CdS layers. Three types of energy distribution were simulated which are single, uniform and Gaussian. For each type of energy distribution, three types of defects were simulated which are neutral, acceptor and donor. Simulations were performed by varying the energy with respect to reference from 0.2 eV to 1.2 eV, the value of the capture cross section hole and electron and the total density.

RESULTS AND DISCUSSION

PARAMETER OF SOLAR CELL

The basic structure of the GeSe solar cell is built in SCAPS-1D. FF takes the optimal value between Voc and Jsc to adapt to the I-V graph. The relationship between FF and Voc and Jsc can be explained by equation (1). Pmp is the optimal power point that can be found between the values of Voc and Jsc. Although the values of Jsc and Voc affect the value of FF, the ratio of changes in the value of Voc being more significant than that of Jsc, Voc becomes the main element that determines the value of FF.

$$FF = \frac{P_{mp}}{V_{oc} \times J_{sc}} \quad (1)$$

The of solar cells is affected by the value of Voc, Jsc, and FF and can be explained by equation (2).

$$\eta = \frac{V_{oc} \times J_{sc} \times FF}{P_{in}} \quad (2)$$

Figure 5 shows a graph of Jsc versus voltage for a baseline model GeSe solar cell. The baseline model GeSe solar cells obtain Voc of 0.62 V, Jsc of 39.52 mA/cm2, FF of 79.34% and η of 19.48%.

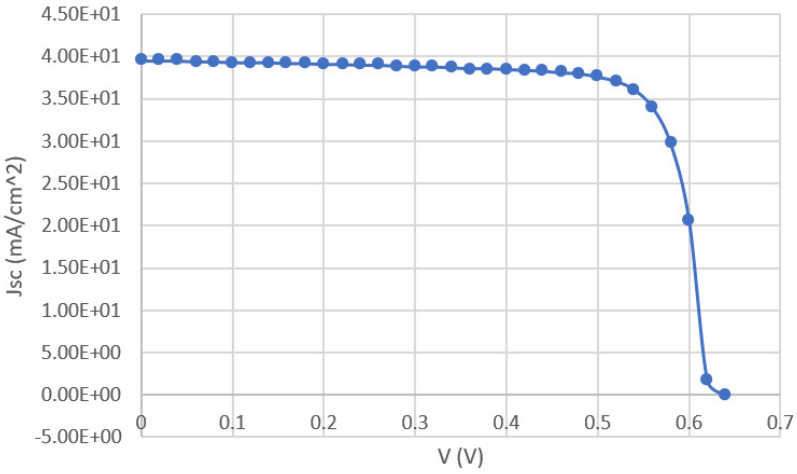

FIGURE 5. Jsc versus voltage graph for a baseline model GeSe solar cell

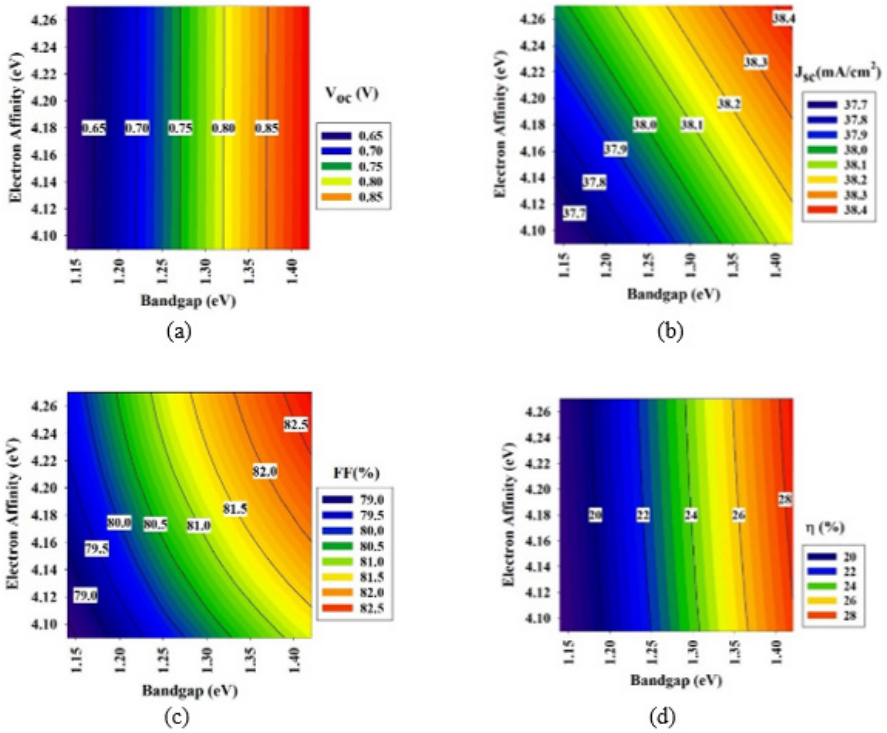

FIGURE 6. Contour plot of electron affinity against bandgap using absorption files extracted from Xue et al. 2016 for (a) Voc, (b) Jsc, (c) FF, (d) η

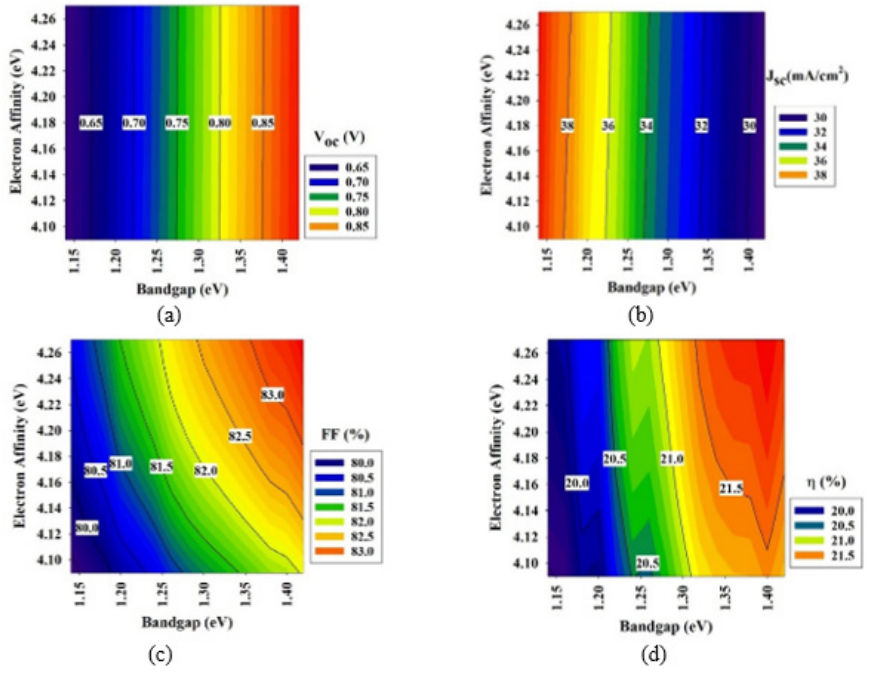

FIGURE 7. Contour plot of electron affinity against bandgap using SCAPS-1D absorption model for (a) Voc, (b) Jsc, (c) FF,FIGURE 8. Contour plots of hole mobility against hole concentration for (a) Voc, (b) Jsc, (c) FF, (d) η

Figure 6 shows the contour plots of electron affinity against bandgap for Voc, Jsc, FF, and η using absorption files extracted from Xue et al. (2016). Based on the observations in Figure 6 (a), Voc is not affected by electron affinity, but an increase in the bandgap leads to an increase in Voc. According to Figure 6 (b), increasing the bandgap and electron affinity results in an increase in Jsc, with lower bandgap values yielding lower Jsc. This finding is contrary to the theory that lower bandgap should yield higher Jsc. Based on Figure 6 (c), increasing the bandgap and electron affinity leads to an increase in FF. Finally, Figure 6 (d) shows that η is not affected by electron affinity, but an increase in the bandgap leads to an increase in η.

Figure 7 shows the contour plots of electron affinity against bandgap for Voc, Jsc, FF, and η using the SCAPS-1D absorption model. Based on Figure 7 (a), Voc is not affected by electron affinity, but an increase in the bandgap leads to an increase in Voc. According to Figure 7 (b), Jsc is not affected by electron affinity, but an increase in the bandgap results in a decrease in Jsc. This finding aligns with the theory that lower bandgap values yield higher Jsc. With a larger bandgap, only high-energy photons can generate hole-electron pairs. However, high-energy photons are less abundant in sunlight compared to low-energy photons. As a result, the reduction in high-energy photons leads to a decrease in the number of hole-electron pairs generated, resulting in lower Jsc. Based on Figure 7 (c), increasing the bandgap and electron affinity leads to an increase in FF. Finally, Figure 7 (d) shows that η is not significantly affected by electron affinity, but an increase in the bandgap leads to an increase in η. The simulated performance of GeSe solar cells using the SCAPS-1D absorption model is more accurate compared to simulations using absorption files extracted from Xue et al. (2016). Therefore, the SCAPS-1D absorption model with a bandgap of 1.40 eV and an electron affinity of 4.27 eV was chosen for further simulations as these values achieved the highest efficiency.

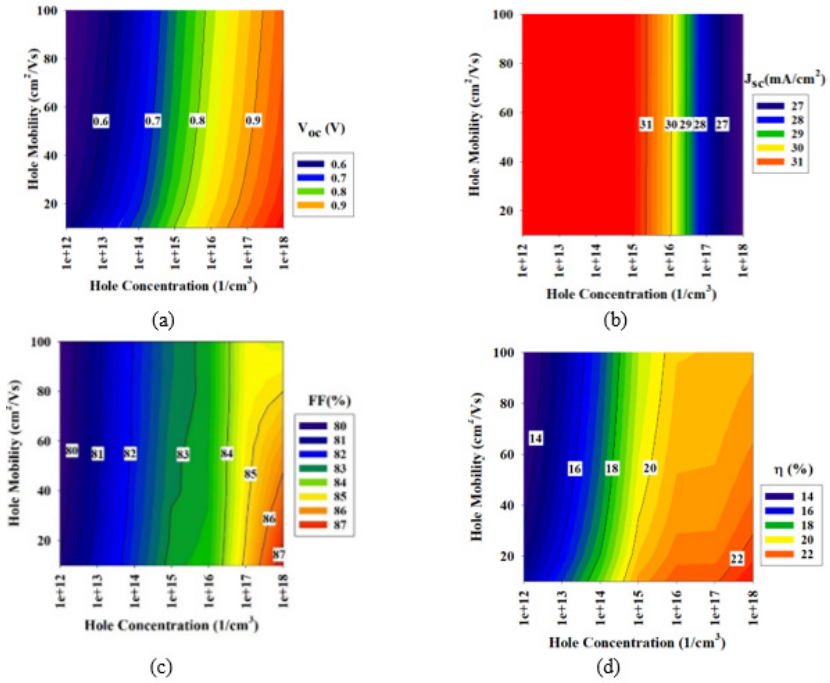

FIGURE 8. Contour plots of hole mobility against hole concentration for (a) Voc, (b) Jsc, (c) FF, (d) η

Figure 8 shows the contour plots of hole mobility against hole concentration for Voc, Jsc, FF, and η. Based on Figure 8 (a), Voc is not significantly affected by hole mobility, but an increase in hole concentration leads to an increase in Voc. According to Figure 8 (b), Jsc is not affected by hole mobility, but an increase in hole concentration results in a decrease in Jsc after reaching 1E+15 1/cm^3. Based on Figure 8 (c), FF is not significantly affected by hole mobility, but an increase in hole concentration leads to an increase in FF. Finally, Figure 8 (d) shows that η is not significantly affected by hole mobility, but an increase in hole concentration leads to an increase in η. The hole mobility of 10 cm^2/Vs and the hole concentration of 1E+18 1/cm^3 were chosen for further simulations.

Figure 9 depicts the thickness of the GeSe layer against Voc, Jsc, FF, and η. Increasing the thickness of the GeSe layer results in higher values of Voc, Jsc, FF, and η. A thickness of 2000 nm for the GeSe layer was selected for further simulations. With this thickness, the GeSe solar cell achieved the optimum η of 26.13%.

According to Smiles et al. (2022), the optimum η is 0.007±0.005% with FTO/CdS/undoped-GeSe/Au configuration. While the simulation demonstrates an impressive efficiency of 26.13% under specific conditions, it's vital to consider real-world challenges. These include variations in material properties, compatibility with manufacturing techniques, economic viability, long-term stability, scalability and defects. Bridging the gap between simulation and practical application requires further research and development efforts to advance thin film solar cell technology and bring these promising results closer to real-world deployment.

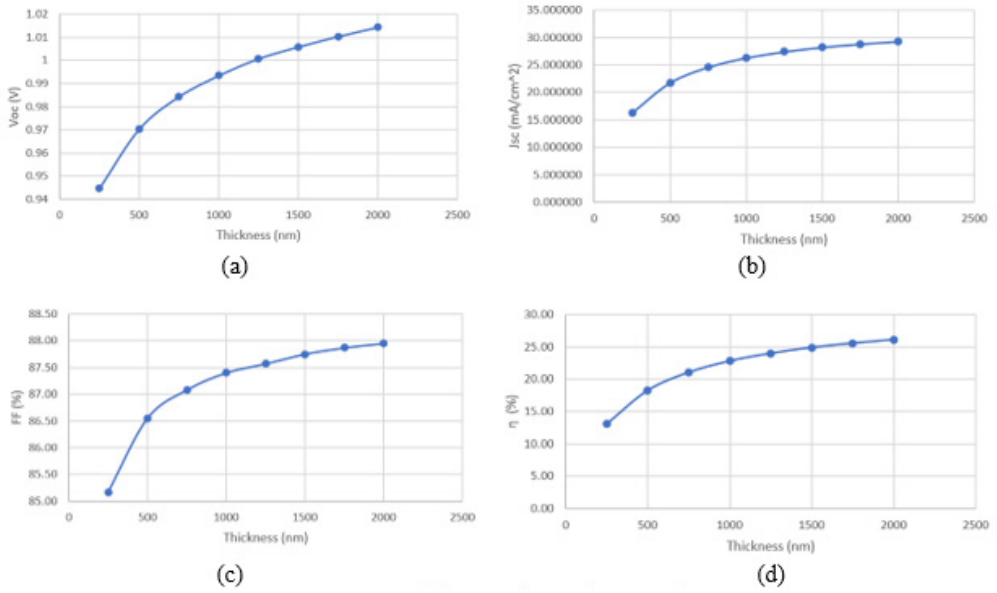

FIGURE 9. Thickness of GeSe layer against
(a) Voc, (b) Jsc, (c) FF, (d) η

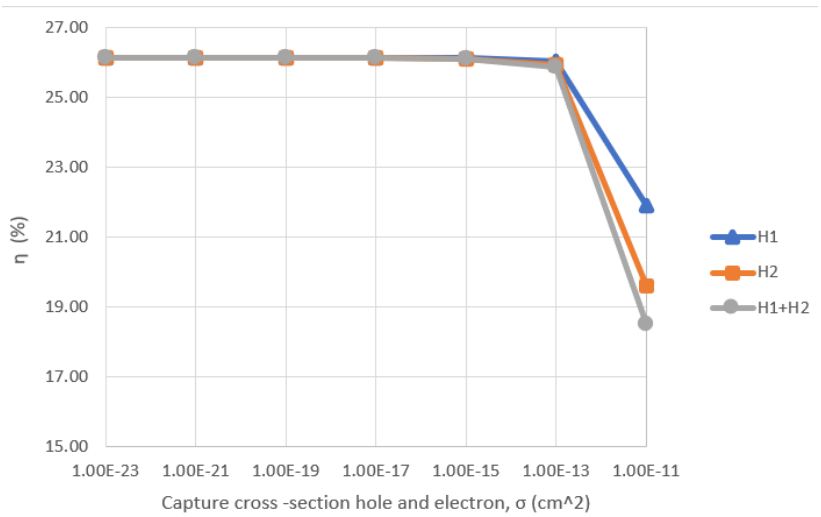

FIGURE 10. Graph of η against σ with N_t values of 1.3E12 1/cm^3 for H1 and 3.0E12 1/cm^3 for H2

DEFECT PROFILES

Three types of bulk defects were simulated, namely Se_{Ge} acceptor defects (H1), Ge_{Se} acceptor defects (H2) and a combination of Se_{Ge} and Ge_{Se} acceptor defects (H1+H2). Figure 10, Figure 11, Figure 12, and Figure 13 respectively show the graph of η against σ with N_t values of 1.3E+12 1/cm^3, 1.3E+14 1/cm^3, 1.3E+16 1/cm^3, 1.3E+18 1/cm^3 for H1, and 3.0E+12 1/cm^3, 3.0E+14 1/cm3, 3.0E+16 1/cm3, 3.0E+18 1/cm3 for H2, respectively. Based on Figure 10, the η of all defects begins to decrease after σ = 1E-13 cm^2. According to Figure 11, the η of all defects begins to decrease after σ = 1E-15 cm^2. In Figure 12, the η for H1 and H2 defects start to decrease after σ = 1E-17 cm^2, whereas the η for H1+H2 defect starts to decrease after σ = 1E-19 cm^2. Based on Figure 13, the η of all defects starts to decrease after σ = 1E-19 cm^2. Overall, increasing N_t and σ will cause η to decrease. The higher the N_t, the lower the σ needed to reduce η.

According to Huang et al. (2023), as N_t is greater than 1E+15 1/cm^3, the η decreases significantly. Both our study and Huang et al. found that increasing Nt has a detrimental effect on solar cell's η. Specifically, as N_t exceeds 1E+15 1/cm3, both studies observed a significant decrease in η. This consistent observation highlights the critical role of N_t in influencing solar cell performance.

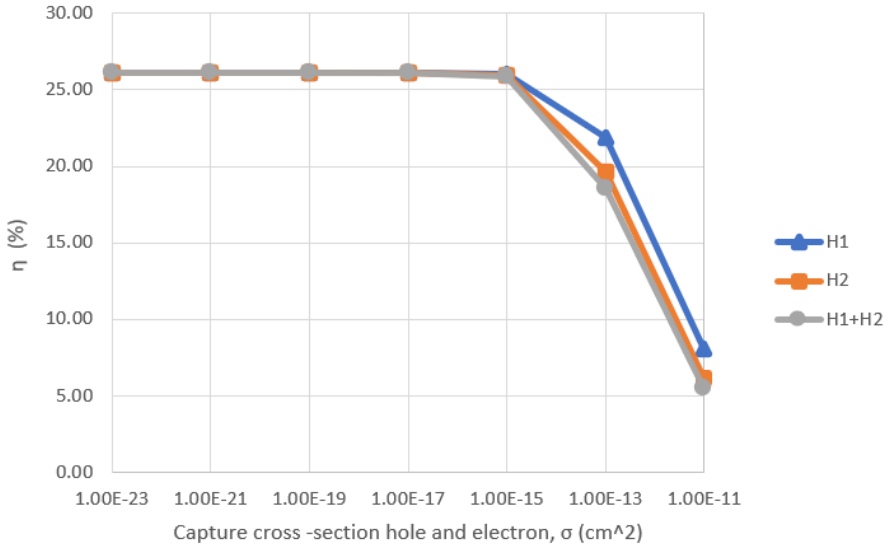

FIGURE 11. Graph of η against σ with N_t values of 1.3E14 1/cm^3 for H1 and 3.0E14 1/cm^3 for H2

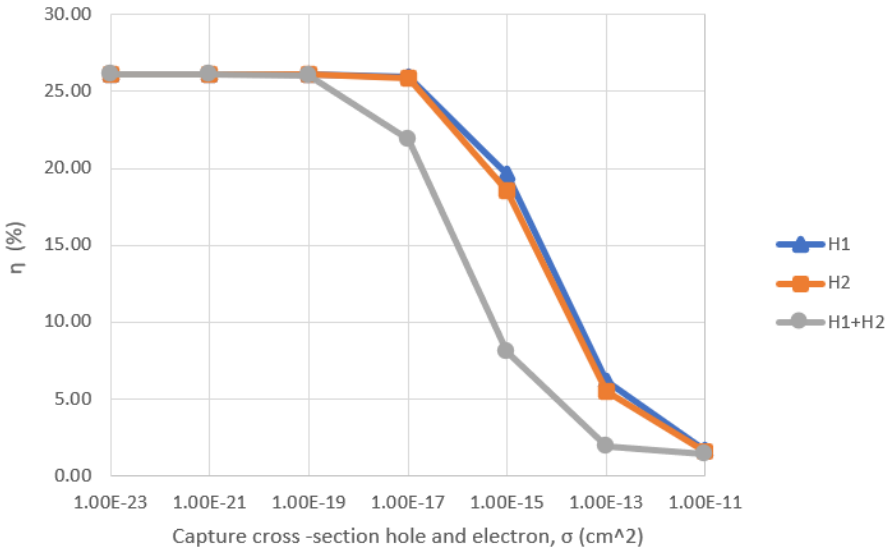

FIGURE 12. Graph of η against σ with N_t values of 1.3E16 1/cm^3 for H1 and 3.0E16 1/cm^3 for H2

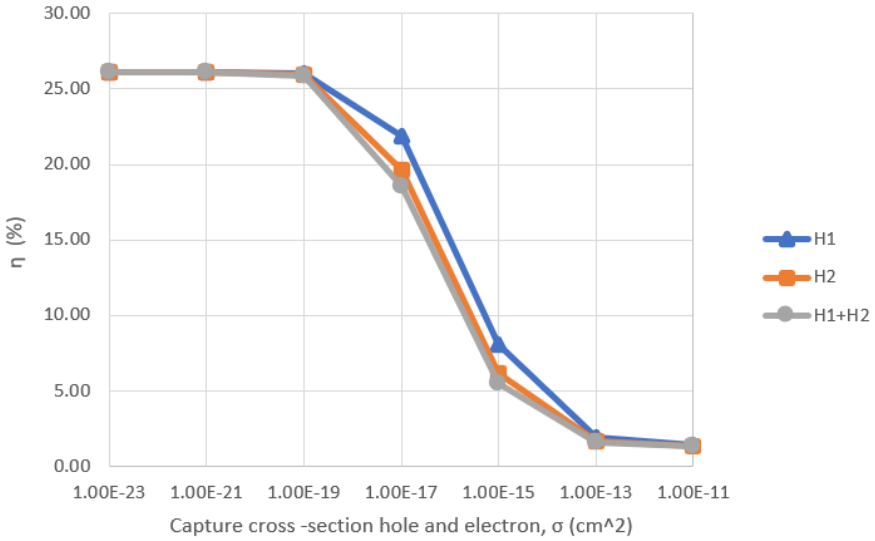

FIGURE 13. Graph of η against σ with N_t values of 1.3E18 1/cm^3 for H1 and 3.0E18 1/cm^3 for H2

Interfacial defect GeSe/CdS was simulated and analyzed. Figure 14, Figure 15, and Figure 16, show the graph of η against energy, respectively, with a total density of 1E+12 1/cm^2 but different σ values of 1E-19 cm^2, 1E-16 cm^2, and 1E-13 cm^2 for single, uniform, and Gaussian energy distributions. Based on Figure 14, the donor defects have increased the solar cell's optimum η for single, uniform, and Gaussian energy distributions when the energy with respect to reference increases. The η remains mostly at 26.13% for neutral and acceptor defects, indicating that these defects have a minimal effect on the solar cell's optimum η. In Figure 15, η decreases compared to Figure 14, and the donor defects have a more significant impact compared to the neutral and acceptor defects. Figure 16 shows the lowest η compared to Figure 14 and Figure 15. Therefore, the total density of 1E+12 1/cm^2 has the most impact at σ of 1E-13 cm^2.

Figure 17, Figure 18, and Figure 19 show the graph of η against energy, respectively, for reference with σ of 1E-19 cm^2 but different total density values of 1E+14 1/cm^2, 1E+16 1/cm^2, and 1E+18 1/cm^2 for single, uniform, and Gaussian energy distributions. Based on Figure 17, the donor defects have increased the solar cell's optimum η for single, uniform, and Gaussian energy distributions at an energy of 1.2 eV. Neutral and acceptor defects slightly reduce the solar cell's optimum η. In Figure 18, η decreases compared to Figure 17. The donor defects have increased the solar cell's optimum η for single, uniform, and Gaussian energy distributions at an energy of 1.2 eV. In Figure 19, the neutral and acceptor defects have a more significant impact compared to the donor defects. Figure 19 shows the lowest η compared to Figure 17 and Figure 18. Therefore, σ of 1E-19 cm^2 has the most impact at a total density of 1E+18 1/cm^2.

Figure 20, Figure 21, and Figure 22 show graph of η against energy, respectively with σ of 1E-16 cm^2 but different total density values of 1E+14 1/cm^2, 1E+16 1/cm^2, and 1E+18 1/cm^2 for single, uniform, and Gaussian energy distributions. Based on Figure 20, all defects have reduced the solar cell's optimum η. In Figure 21, η decreases compared to Figure 20. The neutral and acceptor defects have a more significant impact compared to the donor defects. In Figure 22, η shows a slight decrease compared to Figure 21. The η for the neutral defect remains the same as the energy level increases. For σ of 1E-16 cm^2, the total density of 1E+16 1/cm^2 and 1E+18 1/cm^2 have lower η than the total density of 1E+14 1/cm^2. Therefore, σ of 1E-16 cm^2 has a noticeable impact at the total density of 1E+16 1/cm^2 and 1E+18 1/cm^2.

According to Huang et al. (2023), when interfacial defect densities rise from 1E+10 1/cm^2 to 1E+16 1/cm^2, the η decreases from 17.55% to 13.81%. Comparing our result with Huang et al. (2023), our simulation results align with their observation, which corroborates the detrimental effect of increasing interfacial density densities.

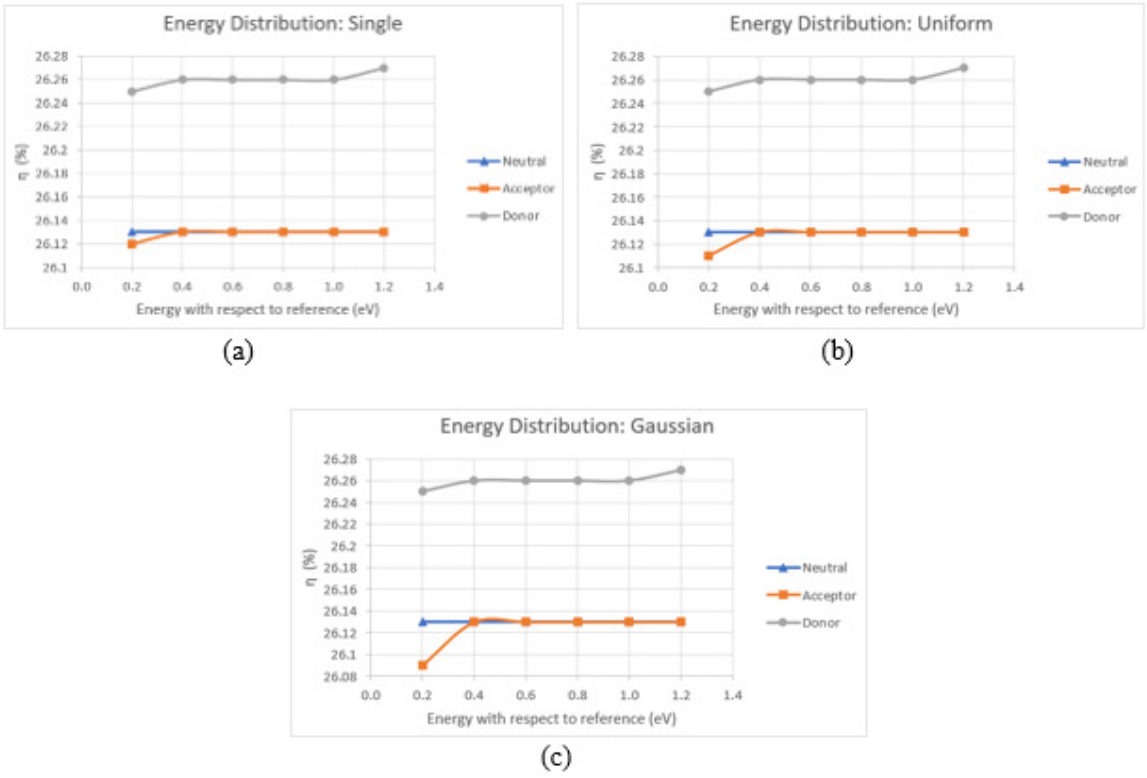

FIGURE 14. Graph of η against energy with respect to reference with total density of 1E+12 1/cm^2 and σ of 1E-19 cm^2 for (a) single, (b) uniform, (c) Gaussian energy distributions

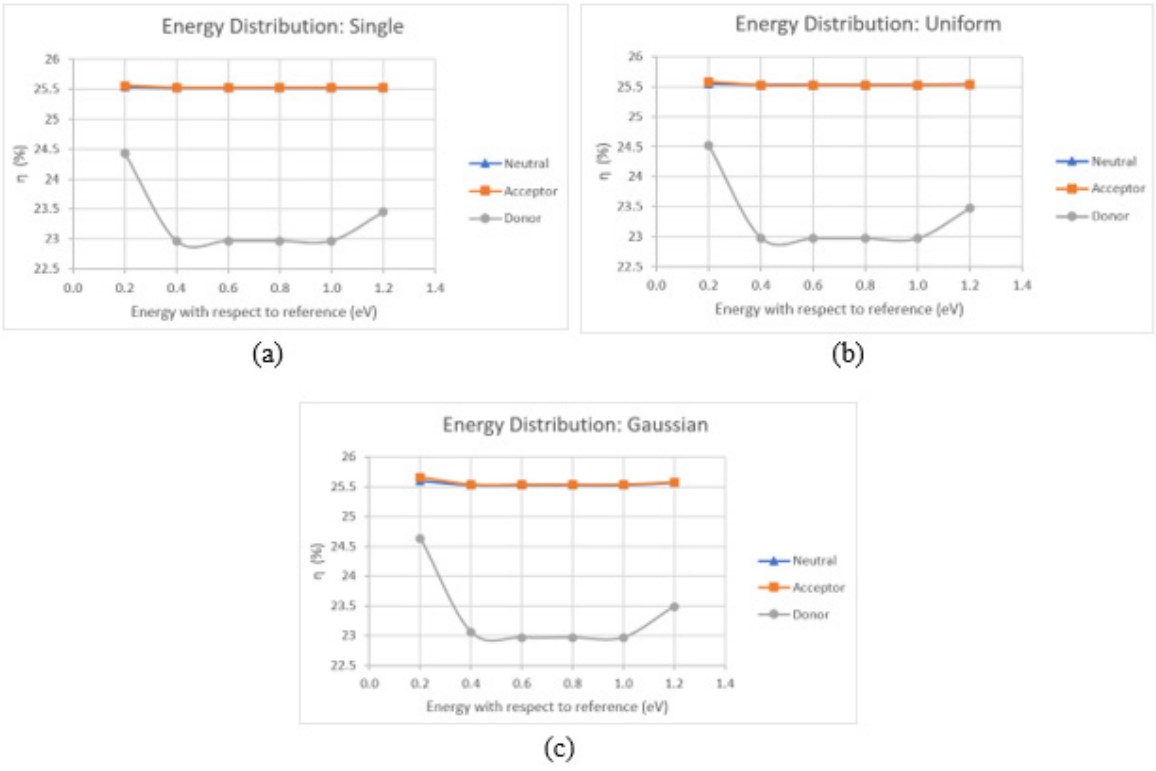

FIGURE 15. Graph of η against energy with respect to reference with total density of 1E+12 1/cm^2 and σ of 1E-16 cm^2 for (a) single, (b) uniform, (c) Gaussian energy distributions

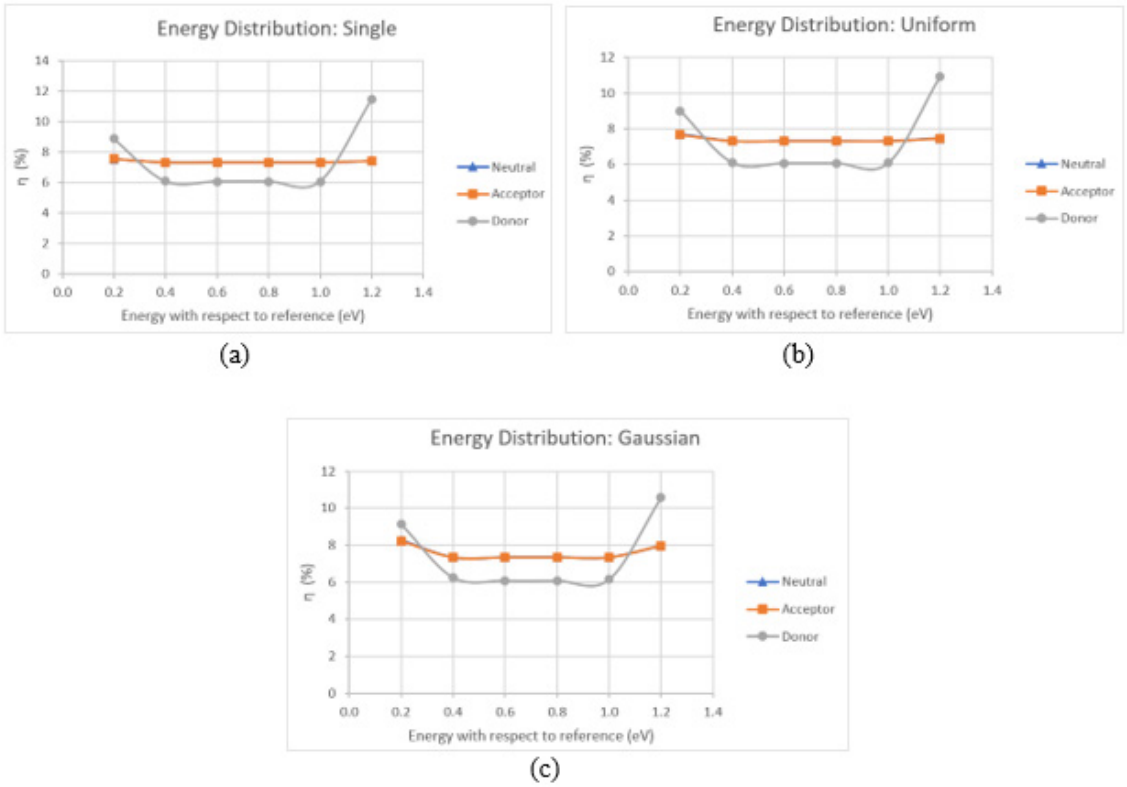

FIGURE 16. Graph of η against energy with respect to reference with total density of 1E+12 1/cm^2 and σ of 1E-13 cm^2 for (a) single, (b) uniform, (c) Gaussian energy distributions

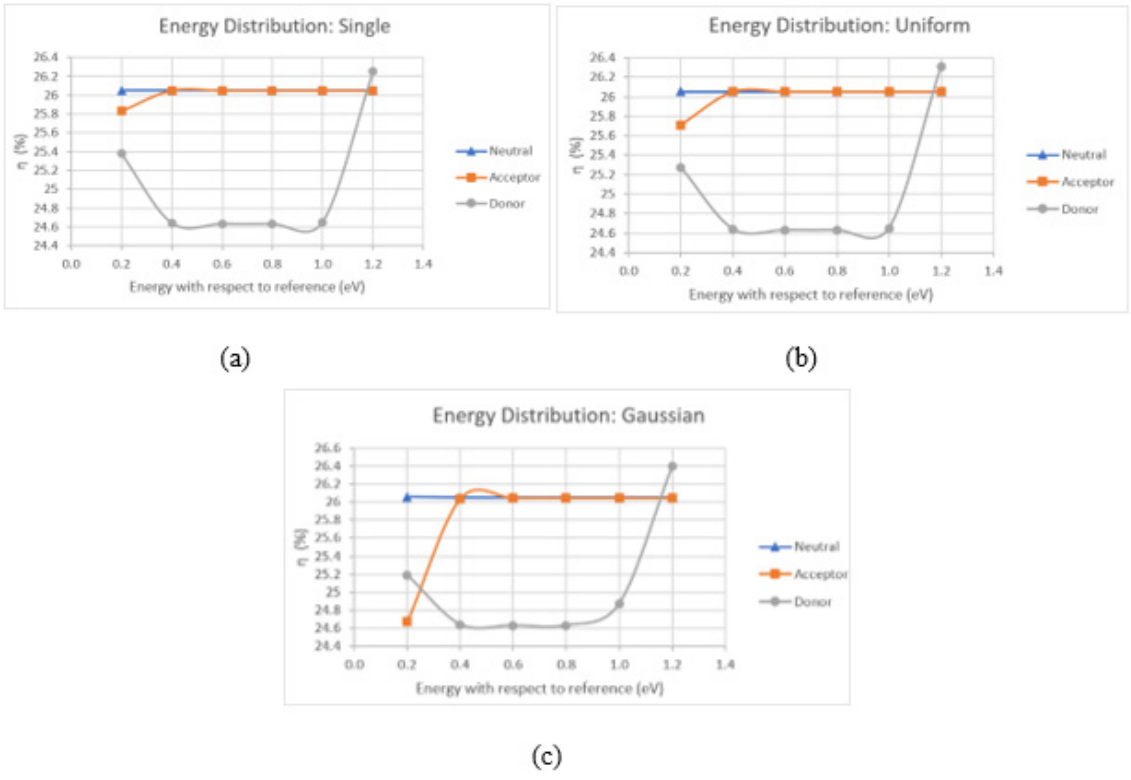

FIGURE 17. Graph of η against energy with respect to reference with total density of 1E+14 1/cm^2 and σ of 1E-19 cm^2 for (a) single, (b) uniform, (c) Gaussian energy distributions

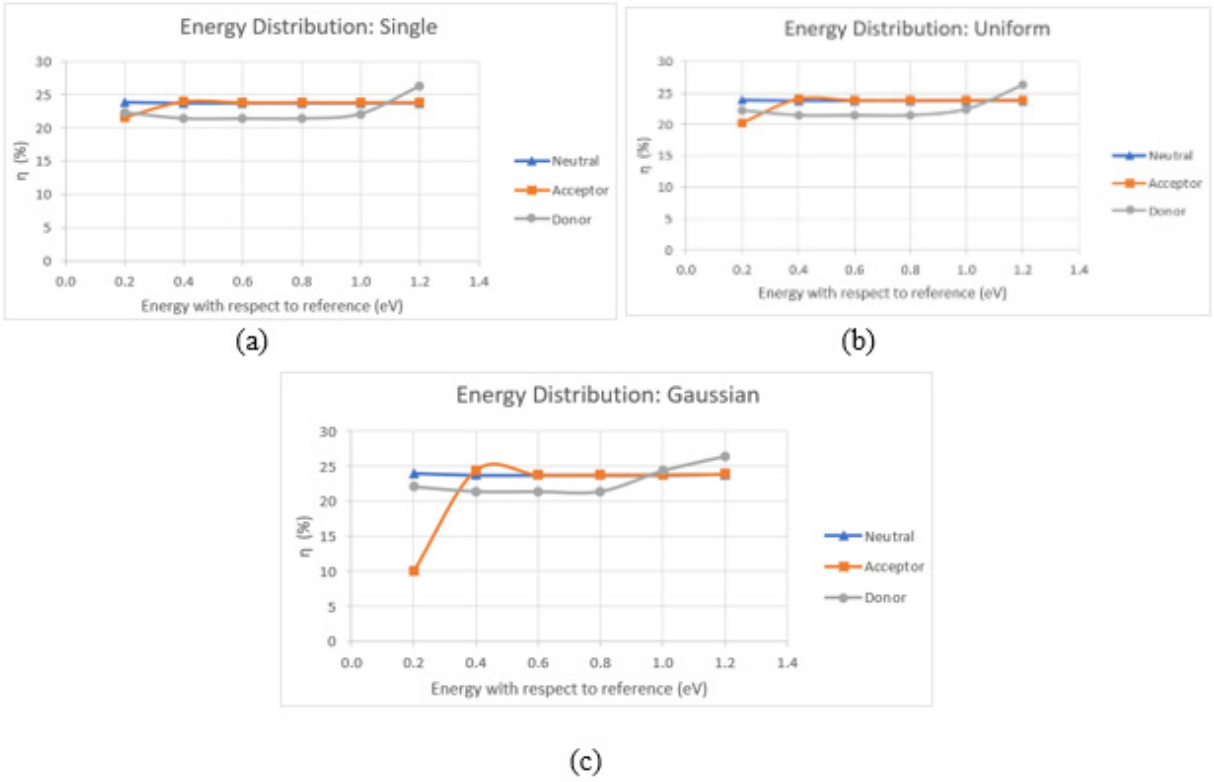

FIGURE 18. Graph of η against energy with respect to reference with total density of 1E+16 1/cm^2 and σ of 1E-19 cm^2 for (a) single, (b) uniform, (c) Gaussian energy distributions

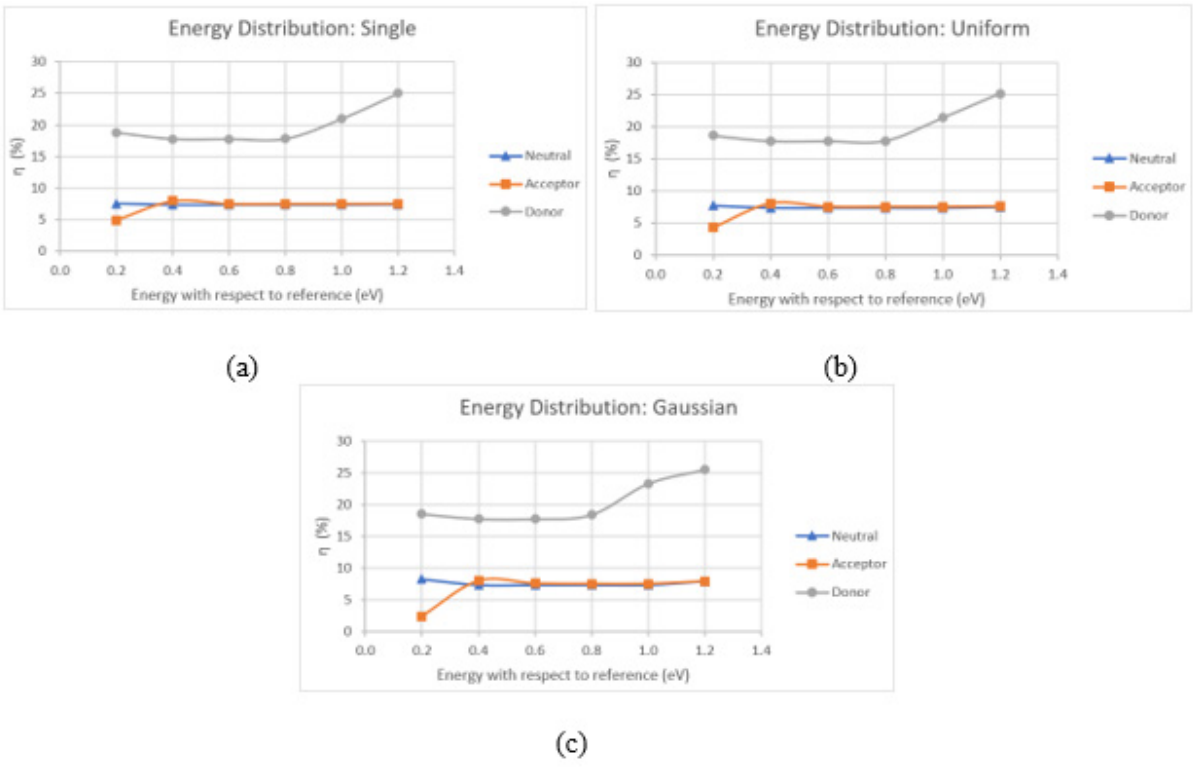

FIGURE 19. Graph of η against energy with respect to reference with total density of 1E+18 1/cm^2 and σ of 1E-19 cm^2 for (a) single, (b) uniform, (c) Gaussian energy distributions

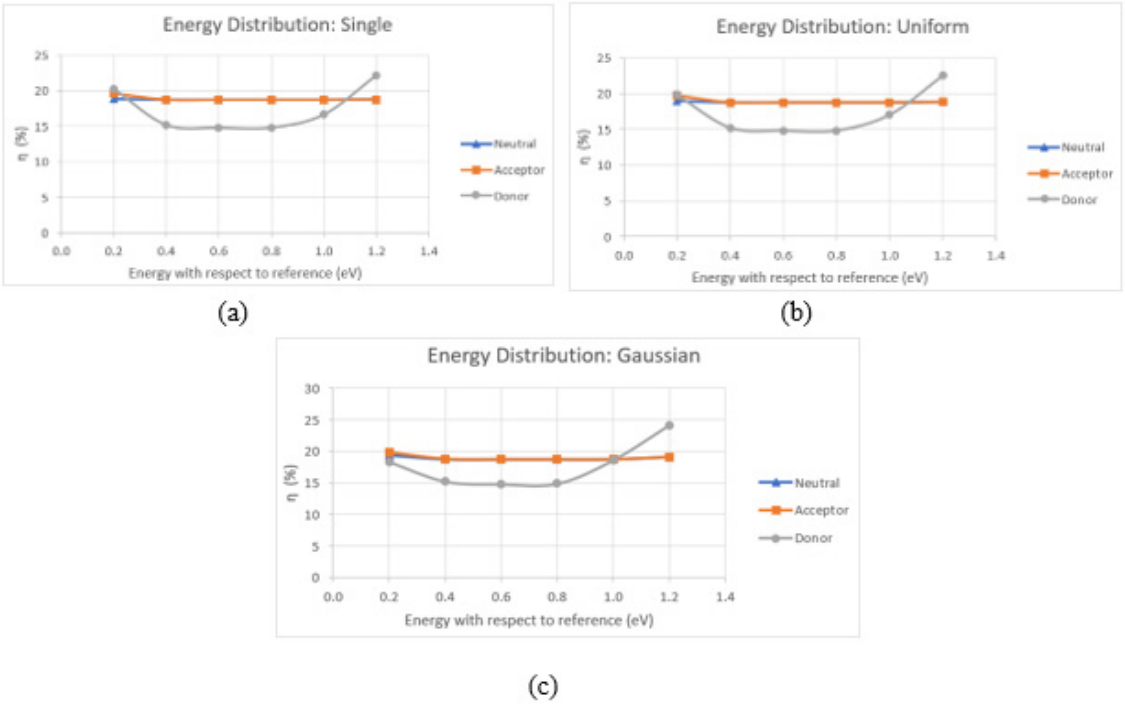

FIGURE 20. Graph of η against energy with respect to reference with total density of 1E+14 1/cm^2 and σ of 1E-16 cm^2 for (a) single, (b) uniform, (c) Gaussian energy distributions

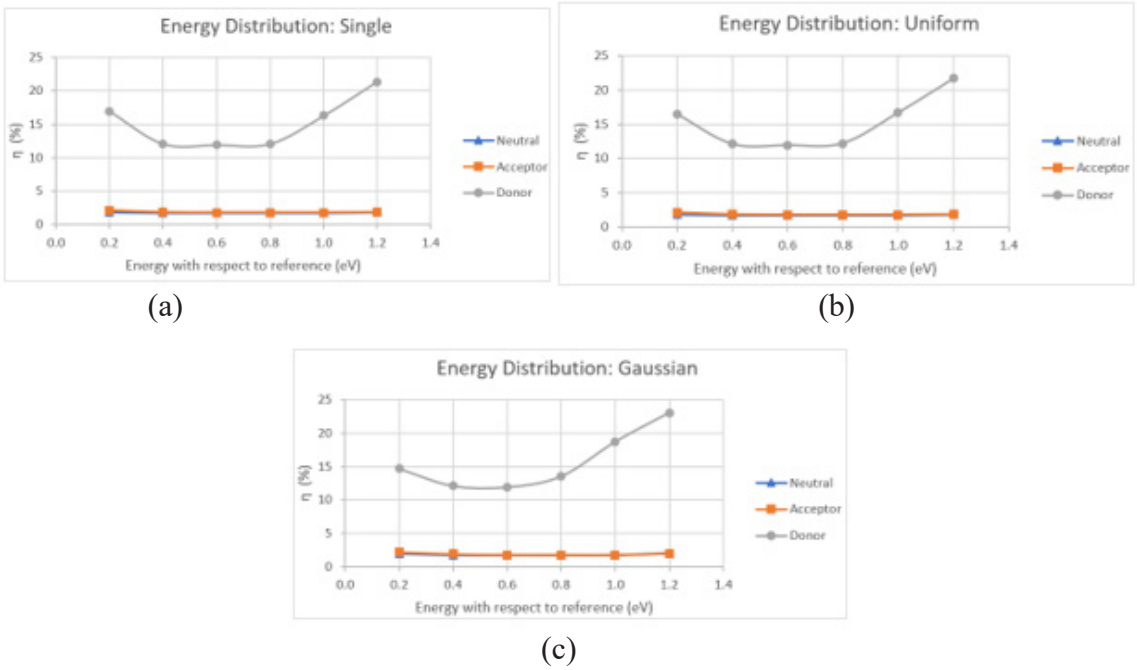

FIGURE 21. Graph of η against energy with respect to reference with total density of 1E+16 1/cm^2 and σ of 1E-16 cm^2 for (a) single, (b) uniform, (c) Gaussian energy distributions

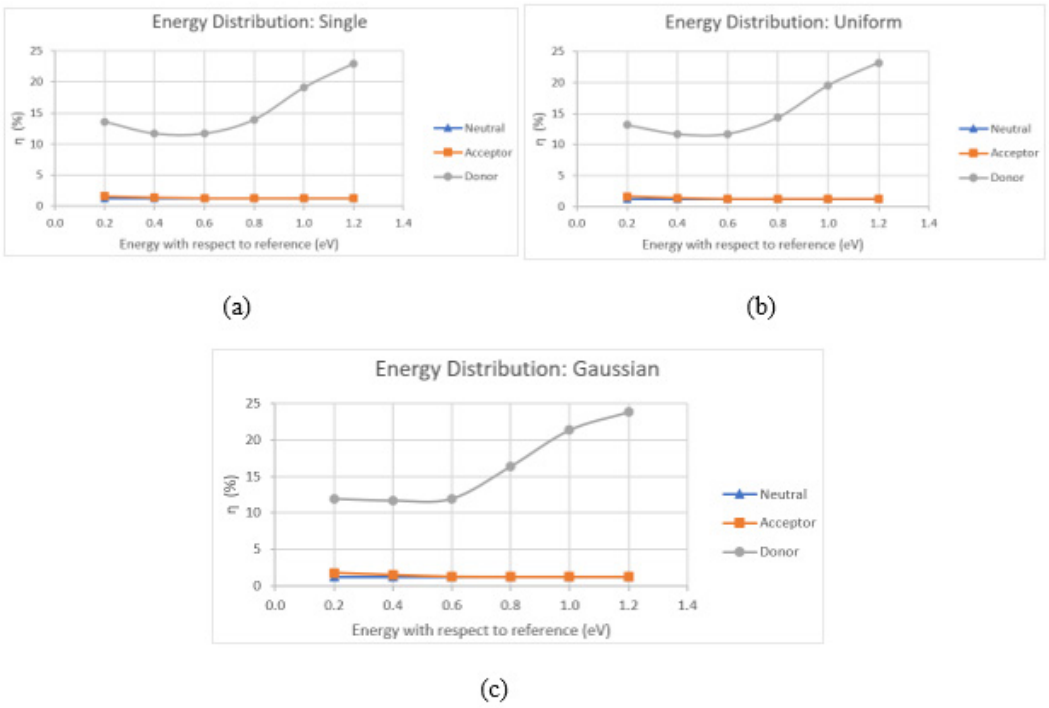

FIGURE 22. Graph of η against energy with respect to reference with total density of 1E+18 1/cm^2 and σ of 1E-16 cm^2 for (a) single, (b) uniform, (c) Gaussian energy distributions

CONCLUSION

Initially, a basic model of GeSe solar cells was constructed and simulated. The simulation obtains Voc of 0.62 V, Jsc of 39.52 mA/cm^2, FF of 79.34%, and η of 19.48%. The simulation was further carried out by varying the bandgap and electron affinity of GeSe, ranging from 1.14 eV to 1.42 eV and 4.09 eV to 4.27 eV, respectively. The simulations were conducted using absorption files extracted from Xue et al. (2016) and the SCAPS-1D absorption model. Results indicated that simulations using the SCAPS-1D absorption model achieved more accurate Jsc contour plots than those using the absorption files extracted from Xue et al. (2016). The SCAPS-1D absorption model with a bandgap of 1.40 eV and an electron affinity of 4.27 eV was selected for further simulations as these values achieved the highest efficiency. Subsequent simulations involved varying the hole mobility from 10 cm^2/Vs to 100 cm^2/Vs and the hole concentration from 1E+12 1/cm^3 to 1E+18 1/cm^3. The hole mobility of 10 cm^2/Vs and the hole concentration of 1E+18 1/cm^3 were chosen for further simulations. Additionally, the thickness of the GeSe layer was varied from 250 nm to 2000 nm, and 2000 nm was selected for further simulations. Using these optimum parameters, the GeSe solar cell achieved an efficiency (η) of 26.13%.

Regarding bulk defects within the GeSe layer, an increase in N_t and σ led to a decrease in η. A larger N_t requires a smaller σ to reduce η. For interfacial defect GeSe/CdS, total density of 1E+12 1/cm^2 with σ of 1E-13 cm^2, total density of 1E+18 1/cm^2 with σ of 1E-19 cm^2, total density of 1E+16 1/cm^2 and 1E+18 1/cm^2 with σ of 1E-16 cm^2 have critical impact to GeSe solar cell. Lower N_t or total density generally requires a higher σ to reduce η. This is because lower N_t would have low strength to capture the carriers, hence needing a larger σ to capture carriers, resulting in a decrease in η.

ACKNOWLEDGEMENT

The authors gratefully acknowledge the Department of Electrical, Electronic, and Systems Engineering and Solar Energy Research Institute of The National University of Malaysia (UKM) for their support and encouragement throughout this study. The authors also would like to acknowledge the Ministry of Higher Education of Malaysia (MOHE) through its research grant FRGS/1/2022/TK08/UKM/02/29. Appreciations are also extended to the Centre for Research and Instrumentation Management (CRIM) of Universiti Kebangsaan Malaysia (UKM).

DECLARATION OF COMPETING INTEREST

None

REFERENCES

Basak, A. & Singh, U.P. 2021. Numerical modelling and analysis of earth abundant Sb_2S_3 and Sb_2S_3 based solar cells using SCAPS-1D. *Solar Energy Materials & Solar Cells* 230: Article number 111184.

Cozza, D., Ruiz, C.M., Duché, D., Simon, J.J. & Escoubas, L. 2016. Modeling the back contact of $Cu_2ZnSnSe_4$ solar cells. *IEEE Journal of Photovoltaics* 6(5): 1292–1297.

Grodzicki, R., Tołłoczko, A.K., Majchrzak, D., Hommel, D. & Kudrawiec, R. 2022. Band alignments of GeS and GeSe materials. *Crystals* 12(10): Article number 1492.

Huang, Z.P., Chen, Y.X., Huang, Z.H., Lin, W.W., Mao, Y., Lin, L.M., Yao, L.Q., Li, H., Cai, L.P. & Chen, G.L. 2023. Simulation of highly efficient GeSe-based solar cells with SCAPS-1D. *Heliyon* 9(8): Article number e18776.

Karl, W.B. & Udo, W.P. 2018. Defects. Dlm W.B. Karl & W.P. Udo (pnyt.). *Semiconductor Physics*, hlm 527-781. Switzerland: Springer International.

Kearney, K., Seo, G., Matsushima, T., Adachi, C., Ertekin, E. & Rockett, A. 2018. Computational analysis of the interplay between deep level traps and perovskite solar cell efficiency. *Journal of the American Chemical Society* 140(46): 15655–15660.

Liu, S.C., Dai, C.M., Min, Y., Proppe, A.H., Zhou, Y., Chen, C., Chen, S., Tang, J., Xue, D.J., Sargent, E.H., Hu, J.S. 2021. An antibonding valence band maximum enables defect-tolerant and stable GeSe photovoltaics. *Nature Communications* 12(1): Article number 670.

Liu, S.C., Li, Z., Wu, J., Zhang, X., Feng, M., Xue, D.J. & Hu, J.S. 2021. Boosting the efficiency of GeSe solar cells by low-temperature treatment of p-n junction. *Science China Materials* 64: 2118–2126.

Liu, S.C., Yang, Y., Li, Z., Xue, D.J. & Hu, S.J. 2020. GeSe thin-fim solar cells. *Materials Chemistry Frontiers* 4(3): 775–787.

Liu, S.C., Mi, Y., Xue, D.J., Chen, Y.X., Liu, X., Hu, J.S. & Wan, L.J. 2017. Investigation of physical and electronic properties of GeSe for photovoltaic applications. *Advanced Electronic Materials* 3(11): Article number 1700141.

Smiles, M.J., Shalvey, T.P., Thomas, L., Hobson, T.D.C., Jones, L.A.H., Phillips, L.J., Don, C., Beesley, T., Thakur, P.K., Lee, T.L., Durose, K., Major, J.D. & Veal, T.D. 2022. GeSe photovoltaics: doping, interfacial layer and devices. *Faraday Discussions* 239: 250-262.

Sze, S.M. & Ng, K.K. 2007. P-N Junction. Dlm. S. M. Sze & K. K. Ng (pnyt.). *Physics of Semiconductor Devices*, hlm. 82-120 Hoboken: Wiley Interscience.

Xue, D.J., Liu, S.C., Dai, C., Chen, S., He, C., Zhao, L., Hu, J.S. & Wan, L.J. 2016. GeSe thin-film solar cells fabricated by self-regulated rapid thermal sublimation. *Journal of the American Chemical Society* 139(2): 958–965.

Yang, Z., Liao, L., Gong, F., Wang, F., Wang, Z., Liu, X., Xiao, X., Hu, W., He, J. & Duan X. 2018. WSe_2/GeSe heterojunction photodiode with giant gate tunability. *Nano Energy* 49: 103–108.

Zeng,C., Zhang, R., Wu, L., Wang, Q., Chen, X. & Lu, P. 2020. Mechanical, electronic and optical properties of bulk and monolayer $GeSe_2$. *International Journal of Modern Physics B* 34(06): Article number 2050034.

Zi, W., Mu, F., Lu, X., Cao,Y., Xie, Y., Fang, L., Cheng, N., Zhao, Z. & Xiao, Z. 2020. Post-annealing treatment of a-GeSe thin films for photovoltaic application. *Solar Energy* 199: 837–843.